DESIGN AND PERFORMANCE TEST OF SPOILER BLADES OF THE DIRECT SEED-METERING DEVICE FOR RICE
/
水稻直播排种器扰流叶片的设计与性能试验

Lin WAN*[1,2], Hongchao WANG[1,2], Gang CHE[1,2], Wensheng SUN[1], Zhengfa CHEN[1] [1]
[1] College of Engineering, Heilongjiang Bayi Agricultural University, Daqing / China;
[2] Key Laboratory of Intelligent Agricultural Machinery Equipment in Heilongjiang Province, Daqing / China
Tel: +86 13555523188; E-mail: wanlin0@yeah.net
DOI: https://doi.org/10.35633/inmateh-68-06

Keywords: *seed-metering device, rice, spoiler blades, design, test*

ABSTRACT
In order to improve air pressure utilization and working performance, the direct seed-metering device for rice was designed with spoiler blades embedded in the air cavity. The study was carried out using theoretical analysis and hydrodynamic methods to obtain the optimum structure of the spoiler blades. Taking the rotating speed of the air cavity, the negative pressure of the air cavity, and the filling height as the test factors, the multiple regression analysis and the response surface analysis were carried out to obtain the best working parameters of the seed-metering device with spoiler blades. The results showed that when the rotating speed of the air cavity was 23.56 r/min, the negative pressure of the air cavity was 4.97 kPa and the filling height was 12.82 cm, the qualified index was 95.21%, the missing index was 3.28% and the multiple index was 1.51%, which was the best seeding performance. Comparing the test with the seed-metering device without spoiler blades, the results showed that the installation of spoiler blades can improve the performance of the seed-metering device under the best working parameters. This study provide a reference for the design of direct seed-metering device for rice.

摘要
为提高气压利用率和工作性能，设计一种在气腔内嵌入扰流叶片的水稻直播排种器。采用理论分析与流体力学方法进行研究，获得了最佳扰流叶片结构。以气腔旋转速度、气腔负压真空度、填种高度为试验因素，进行多元回归分析和响应曲面分析，得到装扰流叶片排种器的最佳作业参数。结果表明当气腔旋转速度为23.56r/min，气腔负压大小为4.97kPa，填种高度为12.82cm时，合格率为95.21%，漏播率为3.28%，重播率为1.51%，排种性能最佳。在最佳工作参数条件下与未安装扰流叶片的排种器进行对比试验，结果表明安装扰流叶片能够提高排种器工作性能。本研究可为水稻直播排种器的设计提供参考。

INTRODUCTION
Rice is one of the main grain crops in China, and it is a staple food for more than half of the global population *(Tian et al., 2022)*. With the acceleration of urbanization and the shortage of rural labor resources, mechanized planting will become an important way of grain production. The level of agricultural machinery in foreign developed countries is relatively high, and rice production has been fully mechanized *(Wan et al., 2019)*. In China, rice is mainly grown in paddy fields, with the main mechanized planting method being machine transplanting *(Chauhan et al., 2015; Yamauchi, 2017)*. Compared with machine transplanting, mechanized direct seeding can reduce the cost without the process of rice transplanting and increase yield per unit area. Therefore, direct seeding of rice is the main development direction for mechanized farming *(Zhang et al., 2018)*.

The performance of the pneumatic seed-metering device decreased due to insufficient utilization of air pressure and the great difference in rice varieties *(Luo et al., 2019; Liu et al., 2018)*. Most scholars use theoretical analysis and structural design methods to solve these problems *(Wu et al., 2020; Yatskul and Lemiere, 2018; Zhang et al., 2021)*. A kind of pneumatic cylinder structure seed-metering device was designed, which can realize the function of one device with multiple rows, and effectively improve the problems of complex pneumatic system and insufficient utilization of air pressure *(Zhang et al., 2015)*.

[1] *Lin Wan, Prof. Ph.D.; Hongchao Wang, Ph.D.; Gang Che, Prof. Ph.D.; Wensheng Sun, Master Degree; Zhenfa Chen, Ph.D.*

According to the principle of side suction seed, a double-cavity structure was designed for rice, which can meet the requirements of direct seeding of conventional rice and hybrid rice. Theoretical analysis of the working process was carried out, and mechanical models were established. The test showed that the seed-metering device has good applicability and uniformity *(Zhang et al., 2016)*.

With the development of computer simulation technology, fluid simulation technology has been more widely used in the research of seed-metering devices. This technology can quantitatively analyze and describe the simulation results *(Li et al., 2021; Gao et al., 2021; Ye et al., 2021)*. With the help of the EDM-CFD simulation method, the working process of the seed-metering device was simulated, and the seed filling performance of different shapes of seeds was analyzed. The design of the seed-metering device was optimized based on the simulation results *(Ding et al., 2018)*. By using the CFD simulation method, the structure of the negative pressure channel was simulated, and the best channel structure was determined. Several independent negative pressure channels control the precision of seed suction, which improves the utilization rate of air pressure and working performance *(Xing et al., 2019)*. At present, a lot of research has been done on the seed-metering device, but few studies have been found on the structure of the air cavity and the flow field in the air cavity of the seed-metering device.

The main objective of this paper is to investigate the effect of different structured spoiler blades on the internal flow field distribution and operating performance of the seeder. The fluent software was used to simulate and analyze the three kinds of spoiler blades, and the optimal structure of the spoiler was determined. The necessity of installing the spoiler blade was verified by a comparative test. A three-factor and the five-level orthogonal experiment was designed to obtain the best working parameters of the pneumatic seed-metering device under the spoiler blades. This study provides guidance and direction for the direct seed-metering device.

MATERIALS AND METHODS

Overall structure and working principle

The direct seed-metering device for rice is mainly composed of spoiler blade, seed-metering plate, directional stirring teeth, and shell, as shown in Fig.1. The negative pressure environment is an enclosed space consisting of a seed-metering plate and base with embedded spoiler blades, rubber brush and bearing. The sprocket is bolted to the base and moves through the drive mechanism, which in turn rotates the air chamber. However, the spoiler blade, rubber brush and bearing remain relatively stationary. Throughout the process, the rice fills the seed storage chamber and is distributed near the suction holes. The rotating process of the air chamber enhances the mobility of the rice by the action of the mixing device, which is more conducive to the adsorption of rice. Depending on the pressure difference between the inside and outside of the air chamber, the rice seeds are sucked onto the seed-metering plate. The scraping adjusting device removes the excess rice seeds and the rubber brush blocks the suction holes. The rice seeds will no longer be sucked by the negative pressure and will fall by its own gravity to the seed delivery tube, ending the seed discharge process.

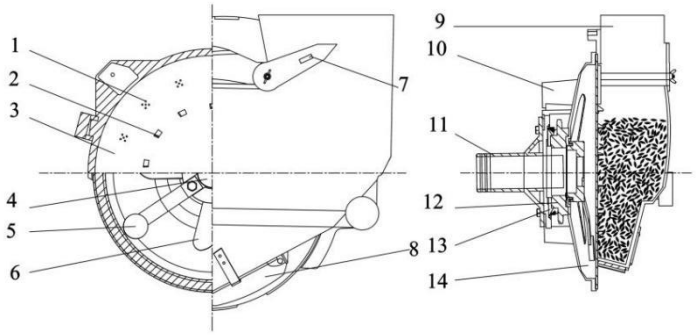

Fig. 1 - Structure of the seed-metering device

1. suction hole; 2. mixing device; 3. seed-metering plate; 4. bearing; 5. rubber brush; 6. spoiler blade; 7. scraping adjusting device; 8. seed unloading device; 9. cover; 10. shell; 11. fan joint; 12. sprocket; 13. washer; 14. base

The spoiler blades

The spoiler blades are installed in the air cavity and rotate relative to the air cavity. As the air chamber turns counterclockwise, the outer ring of the spoiler blades will generate a high linear velocity, driving the surrounding airflow during rotation.

From the simplified Bernoulli's equation, it can be seen that the faster the air flow rate, the lower the pressure, and the larger the air pressure difference at the location of the suction hole, which can improve the air pressure utilization and seed adsorption effect, as shown in equation Eq.(1).

$$p+\rho gh+\frac{1}{2}\rho u^2=C_p \quad (1)$$

Where: p is the pressure (Pa); ρ is the density of the fluid (kg/m^3); g is the acceleration of gravity (m/s^2); h is the height (m); u is the fluid velocity (m/s); C_p is a constant.

The spoiler blades improve the fluidity of the internal flow field of the seed-metering device and increases the pressure difference at the suction holes, thus improving the adsorption performance of the seeds and ensuring that the group of suction holes can evenly absorb the seeds.

Design analysis of three spoiler blade

To investigate the effect of different spoiler blade structures on the internal flow field and the performance of the seed-metering device, three different structures of spoiler blades were designed, as shown in Fig. 2. All three structures were symmetrically distributed in a circular pattern and 3D printed in PLA resin.

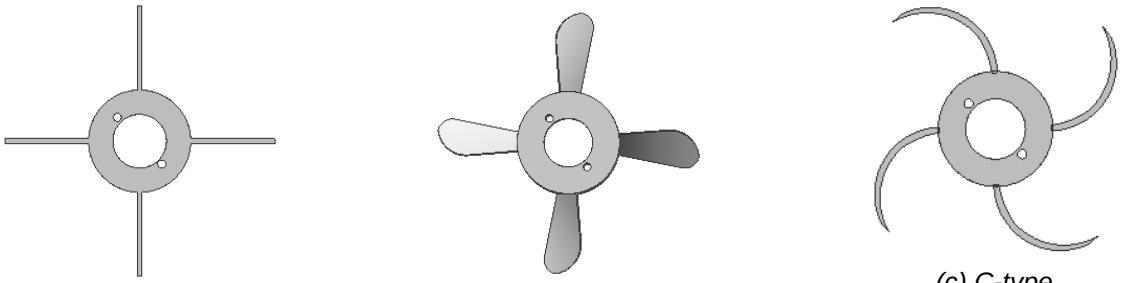

(a) A-type *(b) B-type* *(c) C-type*

Fig. 2 - Structural diagram of three kinds of spoiler blades

The analysis of the three structures of the spoiler blade shows that the A-type spoiler blade is in right-angle contact with the airflow, which has a good spoiler effect, but does not have a significant effect on the airflow guidance. The C-type spoiler blade structure is in right-angle contact with the airflow and has a good inflow effect, but the disturbance effect is not significant. The B-type spoiler blade are designed in a curved form to enhance the flow guidance and contact the airflow at an acute angle, so that the B-type spoiler blades have both flow guidance and spoiler properties. In order to obtain the trajectory of the central air infusion to the outer ring, the starting coordinates of the air mass are assumed to be (R1, 0), and after a period of counterclockwise rotation of the seed-metering plate, the relative equation of motion of the air mass is derived as shown in Eq. (2).

$$\begin{cases} x=R_1\cos(\omega t)-Z\sin(\omega t) \\ y=R_1\sin(\omega t)+Z\cos(\omega t) \end{cases} \quad (2)$$
$$\omega \mathrm{t}\in(0,2\pi)$$

x is the involute abscissa value (mm); y is the involute ordinate value (mm); ω is the angular velocity (rad/s).

The equation shows that the equation of motion of the trajectory of the air mass is an involute with the radius R1 of the base circle. Considering the size of the space in the air cavity and the working efficiency, R1 is designed to be 30 mm and the number of spoiler blade is designed to be 4. To increase the air flow velocity at the group suction holes, the radius of circumferential operation is designed to be 85 mm according to the working principle of the spoiler blade, this position of the suction holes can achieve the best flow velocity and pressure to improve the seeding performance.

Blade design theory

In order to design three types of spoiler blades in a rational way, the analysis of the spoiler blades is based on Schmitz theory. The design of the spoiler blade has to meet the aerodynamic requirements, as illustrated by the B-type spoiler blade. The spoiler blades have an effect on the nearby airflow, causing changes in the flow field within the air cavity and at the cluster suction holes, which can improve the suction performance of the seed-metering device. The air chamber rotates with the sprocket to drive the internal air flow. The spoiler blades come into contact with the air flow inside the chamber and the viscosity of the gas causes a pressure differential to form on the surface of the blades. The forces during the operation of the spoiler blades are shown in Fig. 3.

The simplified formula of L and D is expressed as in the following equation:

$$L = \frac{1}{2}\rho W^2 C_L C dr \tag{3}$$

$$D = \frac{1}{2}\rho W^2 C_D C dr \tag{4}$$

The axial thrust (T) and torque (Q) at the radius of the blade rotation area are shown as follows:

$$dT = N\left(L\cos\phi + D\sin\phi\right) = \frac{1}{2}\rho W^2\left(C_L\cos\phi + C_D\sin\phi\right)KCdr \tag{5}$$

$$dQ = N\left(L\sin\phi - D\cos\phi\right) = \frac{1}{2}\rho W^2 r\left(C_L\sin\phi - C_D\cos\phi\right)KCdr \tag{6}$$

Where: L is the force that raises the blade (N); D is the resistance acting perpendicular to the blade rotation plane (N); C_L is the lift coefficient; C_D is the drag coefficient; ϕ is the inflow angle (°); C is the length of AB (mm); ρ is the air density (kg/m³); W is the relative wind speed (m/s); K is the number of blades; r is the working radius of blade circumference (mm).

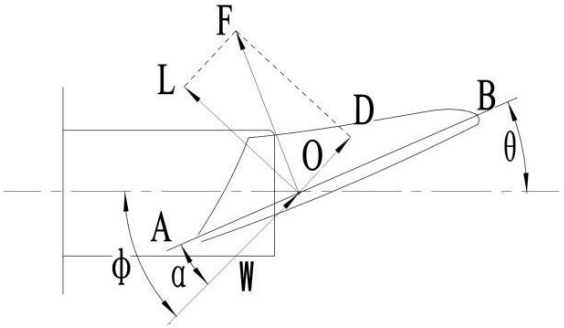

Fig. 3 - Schematic diagram of the spoiler blade

During the relative rotation of the spoiler blades in the air chamber, the pressure on the lower surface is greater than the atmospheric pressure and the pressure on the upper surface is less than the atmospheric pressure, and the airflow at both ends of the blades flows from the high pressure area to the low pressure area. The formation of vortices at the end face of the blade causes the velocity of the flow field corresponding to the group of suction holes to change, increasing the negative pressure difference at the suction holes and improving the seeding performance. Assume that the tangential velocity upstream of the blade is zero and the tangential velocity downstream varies as Δu, as shown in Fig. 4. Then the tangential velocity (U) of the blade is shown as follows:

$$\mathrm{U} = \omega\cdot\mathrm{r} + \frac{\Delta\mathrm{u}}{2} \tag{7}$$

In order to optimize the operating performance of the blades, the value of Δu should be determined by the tip speed ratio of the blades. If friction is neglected and the viscous effect is not considered, the relative speed of the airflow upstream and downstream the blade only changes in direction, and the value does not change.

If the resistance is ignored, the work done by the circumferential force is shown as follows:

$$\mathrm{dP} = \Delta\mathrm{W}\cdot 2\pi\ \rho\mathrm{r}\,\mathrm{dr}\,\mathrm{v}_2\sin\varphi\cdot\mathrm{r}\cdot\omega \tag{8}$$

$$\mathrm{U} = \omega\cdot\mathrm{r} + \frac{\Delta\mathrm{u}}{2}\ \Delta W = 2W_1\sin\left(\phi_1 - \phi\right) \tag{9}$$

$$v_2 = W\sin\phi = W_1\cos\left(\phi_1 - \phi\right)\sin\phi \tag{10}$$

Therefore, the power of the blade is as follows:

$$\frac{\mathrm{dP}}{\mathrm{d}\varphi} = 2\pi\rho\cdot\Omega\cdot\mathrm{r}^2\sin\varphi\cdot\sin\left(2\varphi_1 - 3\varphi\right) = 0 \tag{11}$$

The optimal inflow angle of the relative wind speed is expressed in the following equation:

$$\phi = \frac{2}{3} arcctg\left(\frac{r}{R}\lambda\right) \tag{12}$$

The length of AB and the installation angle of the blade (θ) are expressed in the following equation:

$$C = \frac{16\pi r}{KC_L}\sin^2\left(\frac{arcctg\left(\frac{r}{R}\lambda\right)}{3}\right) \tag{13}$$

$$\theta = \frac{2arcctg\left(\frac{r}{R}\lambda\right)}{3} - \alpha \tag{14}$$

Where: R is the blade spanwise length (mm); α is the angle of attack (°); λ is the blade tip speed ratio.

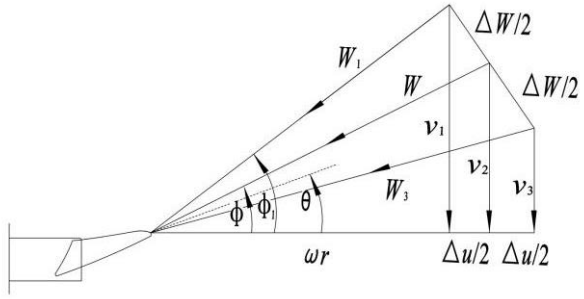

Fig. 4 - Velocity triangles upstream and downstream of the spoiler blade

After theoretical calculation, the installation angle of the spoiler blade is designed as 19° and the length of AB is 51 mm. To consider the working performance and structural balance, the structure coefficient (k_a) can be set, as shown in Fig. 5. The structure coefficient is defined as the ratio of the difference between a certain radius as a reference and the radius of the inner circle, along the direction of increasing blade radius, to the total length of the blade. k_a is expressed in the following equation:

$$k_a = \frac{r_a - r_b}{R} \tag{15}$$

Where: r_a is the radius (mm); r_b is the radius of the inner circle (mm).

The spoiler blades are designed and manufactured as separate components of the seed-metering device and can be delimited by a certain k_a value, divided into an inner and an outer ring along the direction of increasing radius. In order to ensure that the blades have sufficient strength, the blade roots should be kept thick enough. The outer ring of the blade has a high linear velocity, and the Reynolds number of the airflow around the blade is also high, so the curved structure of the blade should be used to increase the gas flow and disturbance, to give full play to the performance of the blade. The k_a =0.5~0.55 range is used as the dividing line, the inner ring area of the blade is dominated by the structural characteristics, the outer ring of the blade is dominated by the maximum air characteristics, so that the design can better maintain the performance of the blade.

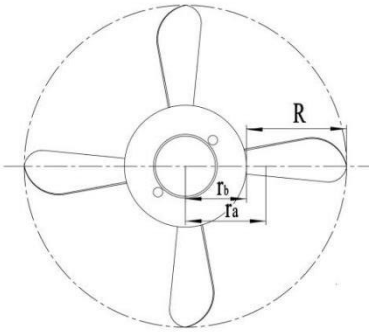

Fig. 5 - Velocity triangles upstream and downstream of the spoiler blade

Experimental material and equipment

The Longjing 31 was selected as the test material. The average moisture content was 22.5% (wet basis) before the test, the weight of 1000 grains was 23.8 g. The experiments were conducted in the Laboratory of Heilongjiang Bayi Agricultural University. The experimental equipment consisted of a belt, motor, rubber tubes, and seed box, as shown in Fig. 6. The direct seed-metering device was installed on a JPS-12 seed-metering device performance test bench. The speed of the locomotive in the field is simulated through the movement of the belt. When the rice falls on the oil belt, the seeds were monitored in real-time through the visual acquisition system. The corresponding data and video were collected to realize the monitoring of the seed-metering process.

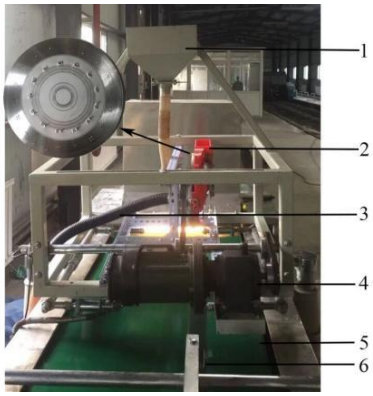

Fig. 6 - Test bench of pneumatic seed-metering device

1. Seed box; 2. seed-metering device; 3. Negative pressure air pipe; 4. Motor; 5. Belt; 6. Oil brush

Experimental design

Simulation test on the flow field of different spoiler blades

According to the structure parameters of the air cavity, the model of the fluid gas cavity was established in the DM module of ANSYS, and the boundary conditions of the inlet, outlet, and wall of airflow were set. The numerical simulations were carried out using an uncoupled implicit solver, choosing the standard k-ε model with an absolute pressure of 101325 Pa. The rotating speed of the air cavity was set at 35 r/min, and the negative pressure of the air cavity was 5 kPa. To quantitatively analyze the simulation effects of the different structures, the average flow velocity data and the average pressure data inside the air cavity for the different sets of suction cross-sections were obtained by means of the post-processing module. To reduce numerical diffusion, a second order windward format was chosen for the calculations and the SIMPLEC algorithm was used for the solution calculations.

Rotation orthogonal combination test

According to the simulation results, the optimal structure of the spoiler blade was selected and applied to the rotation orthogonal combination test. The factor coding levels are shown in Table 1. The optimal combination of parameters was determined through tests, and the interaction between various factors was studied. The experimental design and result are shown in Table 2. In this study, the rotating speed of the air cavity, the negative pressure of the air cavity, and the filling height were represented with codes X_1, X_2, and X_3. The missing index, the qualified index, and the multiple index were taken as output, Y_1, Y_2, and Y_3. According to the actual seeding standard in the field, the qualified index of rice commonly used for direct seeding in holes is 3 to 6 seeds. To ensure the qualified index of operation, agronomic requirements of rice hole diameter is not greater than 50 mm. When the seed-metering device is in a stable state of motion, less than 3 seeds per hole of rice is a missing seed and more than 6 seeds is a reseeding. Each group of experiments was repeated three times, with the average value taken as the test result.

Table 1

Factor level coding table

Code	The rotating speed of the air cavity / r·min^{-1}	The negative pressure of the air cavity / kPa	The filling height / cm
-1.682	14	2.8	6
-1	16.4	3.3	9.6
0	20	4	15
1	23.6	4.7	20.4
1.682	26	5.2	24

RESULTS AND DISCUSSIONS

Analysis of flow field simulation results of different spoiler blades

To study the influence of different structures of the spoiler blade on the internal flow field of the air cavity, the physical model of the corresponding structure was established. Simulation analysis of different structures of spoiler blades was carried out to find the best spoiler blade structure action law. The velocity vector of the flow field in the air cavity was shown in Fig.7.

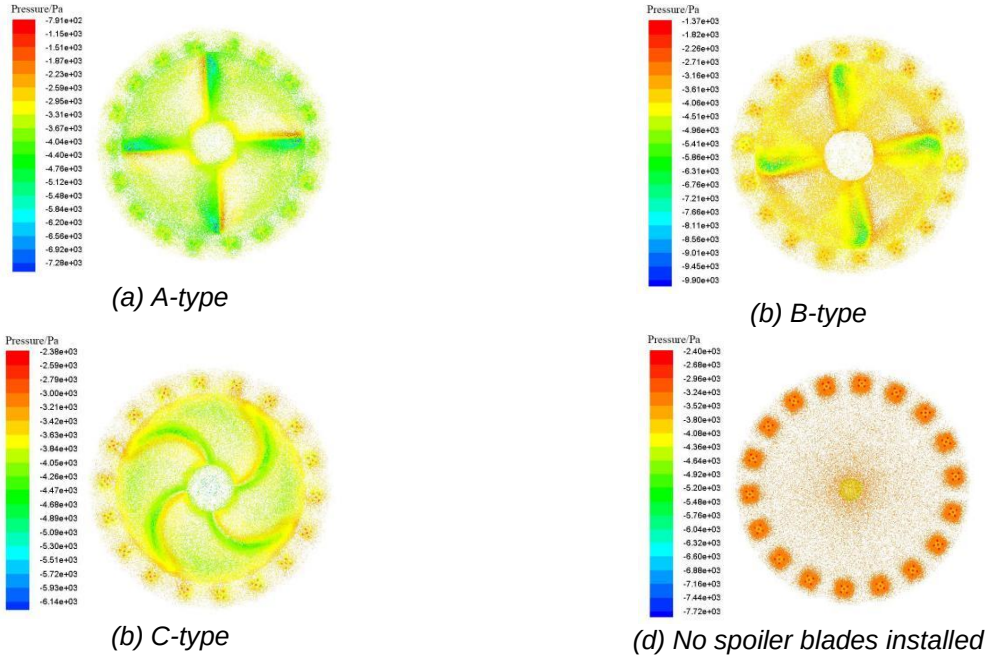

Fig. 7 - Vector diagram of the flow field in the gas cavity

As can be seen from the diagram, the flow field of the different air cavity structures was evenly distributed and stable, with lower pressure values at the group of suction holes than in the surrounding area. The overall pressure and air velocity of the air cavity flow field without the spoiler blade structure was relatively low. In comparison with the simulation of the other three groups of spoiler blades, the spoiler blades can effectively enhance the fluid movement inside the air chamber and increase the air velocity at the group of suction holes, which helps to increase the seed adsorption force and ensure the qualified index. The A-type spoiler blade increase the average pressure inside the air chamber and the air flow velocity at the group of suction holes, but is less effective than B-type and C-type spoiler blades due to the linear structure of the blades and the lack of disturbance. The B-type and C-type were effective in increasing the pressure inside the air chamber and the flow velocity at the suction holes. Due to the curved structure of the B-type and the acute angle of contact with the airflow, the B-type has both inflow and flow disturbance properties. Therefore, a comparative analysis of the structure of the three spoiler blades showed that B-type had a high degree of suitability. The simulation results were consistent with the theoretical analysis. To quantitatively analyze the degree of influence of different spoiler blades on the flow field in the air cavity, the average flow velocity and the average air pressure in the air cavity of different groups of suction hole sections were used as evaluation indicators, and the curves were plotted by processing the simulation data, as shown in Fig. 8.

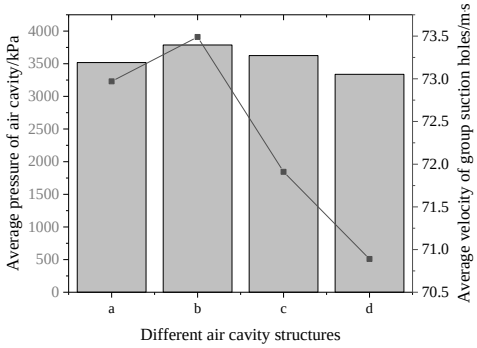

Fig. 8 - Performance curves of different cavity structures

From the simulation results and data graphs, it can be seen that the comprehensive performance of the B-type spoiler blade is optimal, with an average negative pressure of 3787.96 Pa in the air chamber and an average flow velocity of 73.49 m/s at different groups of suction holes, meeting the requirements of direct seeding.

Establishment of the regression model

Multivariate quadratic regression analysis was performed using the Design-Expert software, and the variance analysis of the influence of various factors on evaluating indicators of paddy was obtained, as shown in Table 3. The regression equation of the three groups was highly significant ($p<0.01$). The lack of fit was not significant ($p>0.05$), which indicates the goodness of fit of the regression model. In the results of the variance analysis of the qualified index, the lack of fit P-value was 0.76, indicating that no other factors affect the qualified index. In the results of the variance analysis of the missing index, the lack of fit P-value was 0.11, indicating that no other factors affect the missing index. In the results of the variance analysis of the Multiple index, the lack of fit P-value was 0.06, indicating that no other factors affect the Multiple index. After ensuring that the models were all significant and the misfit terms were not significant, the factor-coded regression equations, excluding the insignificant factors, are shown as follows:

$$Y_1 = 3.9 - 9.37X_2 + 5.57X_1X_3 + 5.51X_1^2 + 8.53X_2^2 \quad (16)$$

$$Y_2 = 92.21 + 4.07X_1 + 6.59X_2 + 7.55X_1X_2 - 10.02X_1^2 - 7.73X_2^2 - 9.72X_3^2 \quad (17)$$

$$Y_3 = 3.89 - 5.19X_1 + 2.79X_2 - 6.64X_1X_2 + 4.51X_1^2 + 6.6X_3^2 \quad (18)$$

By analyzing the result and the P-values of various factors, the effects of these factors on Y_1 ranks in the order: $X_1>X_2>X_3$; on Y_2 ranks in the order: $X_2>X_1>X_3$; in terms of the effect on Y_3 ranks in the order: $X_2>X_1>X_3$.

Table 2

Test scheme and results

Group	X_1	X_2	X_3	Y_1/%	Y_2/%	Y_3/%
1	1	1	1	6.46	88.43	5.11
2	1	1	-1	1.51	95.47	3.02
3	1	-1	1	15.47	81.37	3.16
4	1	-1	-1	14.48	78.58	6.94
5	-1	1	1	4.94	82.84	12.22
6	-1	1	-1	7.9	79.46	12.64
7	-1	-1	1	12.56	83.12	4.32
8	-1	-1	-1	19.71	76.36	3.93
9	1.682	0	0	13.63	84.45	1.92
10	-1.682	0	0	3.84	77.84	18.32
11	0	1.682	0	1.74	91.25	7.01
12	0	-1.682	0	21.85	75.74	2.41
13	0	0	1.682	5.84	83.96	10.2
14	0	0	-1.682	6.84	78.94	14.22
15	0	0	0	6.49	91.74	1.77
16	0	0	0	4.83	92.25	2.92
17	0	0	0	2.94	93.83	3.23
18	0	0	0	3.83	93.83	2.34
19	0	0	0	2.63	94.95	2.42
20	0	0	0	2.85	94.37	2.78
21	0	0	0	1.94	91.87	6.19
22	0	0	0	2.04	92.78	5.18
23	0	0	0	7.78	84.64	7.58

Model interaction item analysis

The qualified index was an important index to evaluate the performance of the direct seed-metering device. Therefore, the research focuses on the analysis of the interaction of various factors on the qualified index, and the response surface was shown in Fig. 9. Figure 9(a) represents the interactive effect of the rotating speed and the negative pressure of the air cavity on the qualified index when the filling height was 15 cm. When the rotating speed of the air cavity was fixed, the qualified index gradually rose with increasing the negative pressure of air cavity, reached a maximum, and then slowly dropped down. When the negative pressure of the air cavity was fixed, the qualified index also gradually rose with increasing the rotating speed of air cavity, reached a maximum, and then slowly dropped down.

The negative pressure of the air cavity had a range of 4.8~5.0 kPa, the rotating speed of the air cavity had a range of 22~24 r/min and the qualified index was optimal. Fig. 9(b) represents the rotating speed of air cavity which was 20 r/min and the interactive effect between the negative pressure of the air cavity and the filling height on the qualified index. When the filling height was fixed, the qualified index gradually rose with increasing the negative pressure of the air cavity, reached a maximum, and then slowly dropped down. When the negative pressure of the air cavity was fixed, the qualified index gradually rose with increasing the filling height, reached a maximum, and then slowly dropped down. The negative pressure of the air cavity had a range of 4.5~4.7 kPa, the filling height had a range of 14~16 cm and the qualified index was optimal. Fig. 9(c) represents the negative pressure of the air cavity which was 4 kPa and the interactive effect between the filling height and the rotating speed of air cavity on the qualified index. When the filling height was fixed, the qualified index gradually rose with increasing the rotating speed of air cavity, reached a maximum, and then slowly dropped down. When the rotating speed of the air cavity was fixed, the qualified index gradually rose with increasing the filling height, reached a maximum, and then slowly dropped down. The rotating speed of the air cavity had a range of 20~22 r/min, the filling height had a range of 14~16 cm and the qualified index was optimal.

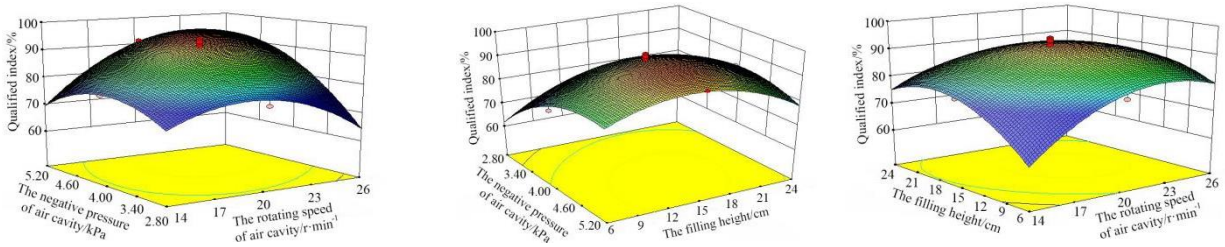

(a) (b) (c)

Fig. 9 - Performance curves of different cavity structures

Table 3

Results of the variance analysis

Source	Missing index			Qualified index			Multiple index		
	Sum of squares	F value	p-value	Sum of squares	F value	p-value	Sum of squares	F value	p-value
Model	684.4	11.2	<0.01	904.7	13.1	<0.01	349.6	4.99	<0.01
X_1	6.14	0.91	0.3	80.76	10.5	< 0.01	131.4	16.9	< 0.01
X_2	414.9	61.3	<0.01	205.1	26.7	< 0.01	36.56	4.7	< 0.01
X_3	2.51	0.37	0.55	14.99	1.95	0.18	5.23	0.67	0.42
X_1X_2	0.81	0.12	0.73	55.81	7.27	*	43.15	5.55	< 0.05
X_1X_3	32.2	4.76	< 0.05	25.88	3.37	0.08	0.34	0.04	0.83
X_2X_3	8.3	1.23	0.28	21.81	2.84	0.11	3.2	0.41	0.53
X_1^2	60.7	8.98	< 0.05	200.9	26.1	< 0.05	40.71	5.23	< 0.05
X_2^2	142.4	21.0	< 0.05	116.8	15.2	< 0.05	1.27	0.16	0.69
X_3^2	19.4	2.87	0.11	188.9	24.6	< 0.05	87.1	11.2	< 0.05
Residual	87.99			99.76			101.1		
lack of fit	54.43	2.59	0.11	24.39	0.52	0.76	68.95	3.43	0.06
Pure error	33.56			75.37			32.2		
Sum	772.4			1004.5			450.7		

From the above analysis, every time the interaction among factors affects the performance of the direct seed-metering device. Optimized parameters were defined by the Design-Expert software version 8.0.6-trail. When the rotating speed of the air cavity was 23.56 r/min, the negative pressure of the air cavity was 4.97 kPa, and the filling height was 12.82 cm, the direct seed-metering device has the overall best performance.

The contrast tests of five groups were carried out according to the optimal parameter combination. The results showed that the performance of the direct seed-metering device can be improved by installing the spoiler blade, as shown in Table 4, which proves the necessity of installing spoiler blades.

Table 4

Contrast test results

Types	Evaluation index		
	Qualified index / %	Missing index / %	Multiple index / %
Spoiler blade installed	93.9	3.6	2.5
No spoiler blade installed	90.5	5.8	3.7

CONCLUSIONS

(1) To further improve the performance of the direct seed-metering device, three spoiler blades with different structures were designed. Through theoretical analysis, it is concluded that the spoiler with a larger upwind angle and curved structure has a better effect on airflow guidance and disturbance.

(2) The CFD method was used to simulate the effect of three different structured spoiler blades on the internal flow field of the direct seed-metering device, and it was concluded that all three types of spoiler blades can improve the flow field. The simulation data showed that the average air pressure in the flow field and the average flow velocity at the suction hole of the B-type spoiler blade were more favorable to the operation, which concluded that the B-type was the most effective.

(3) By optimizing the experimental data, the optimum parameters of the direct seed-metering device are as follows: the rotating speed of the air cavity, 23.56 r/min; the negative pressure of the air cavity, 4.97 kPa; and the filling height, 12.82 cm. Under these conditions, the qualified index is 95.21%, the missing index is less than 3.28% and the multiple index is less than 1.51%.

ACKNOWLEDGEMENT

This work was supported by the National Key R&D Program of China (Grant No. 2018YFD0700601-03); Heilongjiang Bayi Agricultural University Support Program for San Heng San Zong (Grant No. ZRCPY202012); Heilongjiang Bayi Agricultural University Mechanical Engineering Discipline Project.

REFERENCES

[1] Ding, L., Yang, L., Wu, D., Li, D., Zhang, D., & Liu, S. (2018). Simulation and Experiment of Corn Air Suction seed-metering Device Based on DEM-CFD Coupling Method. *Transactions of the Chinese Society for Agricultural Machinery*, vol.49, no.11, pp.48-57.

[2] Farooq, M., Siddique, K. H., Rehman, H., Aziz, T., Lee, D. J., & Wahid, A. (2011). Rice direct seeding: Experiences, challenges, and opportunities. *Soil & Tillage Research*, vol.111, no.2, pp.87-98.

[3] Gao, X., Cui, T., Zhou, Z., Yu, Y., & Song, W. (2021). DEM study of particle motion in novel high-speed seed metering device. *Advanced Powder Technology*, vol.32, no.5, pp.1438-1449.

[4] Li, Z., Zhang, P., Sun, y., Zheng, C., Xu, L., & E, DY. (2021). Discrete particle simulation of gas-solid flow in air-blowing seed metering device. *Computer Modeling in Engineering & Sciences*, vol.127, no.3, pp.1119-1132.

[5] Liu, Q., Cui, T., Zhang, D., Yang, L., Wang Y., He, X., & Wang, M. (2018). Design and experimental study of seed precise delivery mechanism for high-speed maize planter. *International Journal of Agricultural and Biological Engineering*, vol.11, no.4, pp.81-87.

[6] Luo, X., Wang, Z., Zeng, S., Zang, Y., Yang, W., & Zhang, M. (2019). Research progress on mechanized direct seeding technology of rice. *Journal of South China Agricultural University*, vol.40, no.5, pp.1-13.

[7] Tian, L., Ding, Z., Su, Z., Li, L., & Wang, Z. (2022). Design and experiment of rotary precision hill direct seed-metering device for rice. *INMATEH Agricultural Engineering*, vol.66, no.1, pp.311-320.

[8] Wan, L., Wang, H., & Che, G. (2019). Design and Test of Rice Hill-drop seed-metering Device Embedded with Rotating Air Cavity. *Transactions of the Chinese Society for Agricultural Machinery*, vol.50, no.11, pp.74-84.

[9] Wu, Z., Li, M., Lei, X., Wu, Z., Jiang, C., Zhou, L., & Chen, Y. (2020). Simulation and parameter optimization of a centrifugal rice seeding spreader for a UAV. *Biosystems Engineering*, vol.192, pp.275-293.

[10] Xing, H., Zang, Y., Wang, Z., Luo, X., Pei, J., He, S., Xu, P., & Liu, S. (2019). Design and parameter optimization of rice pneumatic seeding metering device with adjustable seeding rate. *Transactions of the CSAE*, vol.35, no.4, pp.20-28.
[11] Yamauchi, M. (2017). A review of iron-coating technology to stabilize rice direct seeding onto puddled soil. *Agronomy Journal*, vol.109, no.3, pp.739-750.
[12] Yatskul. A., & Lemiere, J. (2018). Establishing the conveying parameters required for the air-seeders. *Biosystems Engineering*, vol.166, pp.1-12.
[13] Ye, S., Zheng, D., Li, W., Lu, Q., Yang, Y., Liu, Y., & Xu, B. (2021). Characterization and CFD-DEM modelling of a prismatic spouted bed. *INMATEH Agricultural Engineering*, vol.64, no.2, pp.185-194.
[14] Zhang, G., Zhang, S., Yang, W., Lu, K., Lei, Z., & Yang, M. (2016). Design and experiment of double cavity side-filled precision hole seed-metering device for rice. *Transactions of the CSAE*, vol.32, no.8, pp.9-17.
[15] Zhang, M., Wang, Z., Luo, X., Zang, Y., Yang, W., & Xing, H. (2018). Review of precision rice hill-drop drilling technology and machine for paddy. *International Journal of Agricultural and Biological Engineering*, vol.11, no.3, pp.1-11.
[16] Zhang, S., Xia, J., Zhou, Y., Zhai, J., Guo, Y., Zhang, X., & Wu, H. (2015). Design and experiment of pneumatic cylinder-type precision direct seed-metering device for rice. *Transactions of the CSAE*, vol.31, no.1, pp.11-19.
[17] Zhang, X., Zhu, D., Xue, K., Li, L., Zhu, j., Zhang, S., & Liao, J. (2021). Parameter Optimization and Experiment of Slider-Hole-Wheel Seed-metering Device Based on Discrete Element Method. *INMATEH Agricultural Engineering*, vol.65, no.3, pp.410-420.